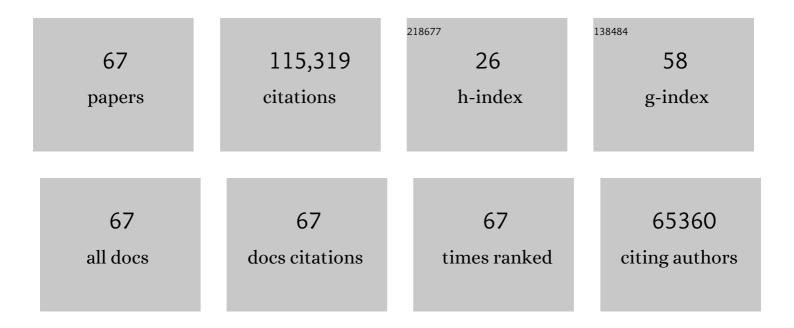
List of Publications by Year in descending order

Source: https://exaly.com/author-pdf/1055886/publications.pdf Version: 2024-02-01



IIAN SUN

#	Article	IF	CITATIONS
1	Deep Residual Learning for Image Recognition. , 2016, , .		100,885
2	Delving Deep into Rectifiers: Surpassing Human-Level Performance on ImageNet Classification. , 2015, , .		9,828
3	Guided Image Filtering. Lecture Notes in Computer Science, 2010, , 1-14.	1.3	819
4	Lazy snapping. ACM Transactions on Graphics, 2004, 23, 303-308.	7.2	807
5	ADMM-CSNet: A Deep Learning Approach for Image Compressive Sensing. IEEE Transactions on Pattern Analysis and Machine Intelligence, 2020, 42, 521-538.	13.9	439
6	Gradient Profile Prior and Its Applications in Image Super-Resolution and Enhancement. IEEE Transactions on Image Processing, 2011, 20, 1529-1542.	9.8	285
7	Proximal Dehaze-Net: A Prior Learning-Based Deep Network for Single Image Dehazing. Lecture Notes in Computer Science, 2018, , 729-746.	1.3	184
8	Multimodal 2D+3D Facial Expression Recognition With Deep Fusion Convolutional Neural Network. IEEE Transactions on Multimedia, 2017, 19, 2816-2831.	7.2	160
9	Atmospheric levels and cytotoxicity of polycyclic aromatic hydrocarbons and oxygenated-PAHs in PM2.5 in the Beijing-Tianjin-Hebei region. Environmental Pollution, 2017, 231, 1075-1084.	7.5	119
10	BM3D-Net: A Convolutional Neural Network for Transform-Domain Collaborative Filtering. IEEE Signal Processing Letters, 2018, 25, 55-59.	3.6	117
11	A Graph-Based Semisupervised Deep Learning Model for PolSAR Image Classification. IEEE Transactions on Geoscience and Remote Sensing, 2019, 57, 2116-2132.	6.3	109
12	Chemical profiles of urban fugitive dust PM2.5 samples in Northern Chinese cities. Science of the Total Environment, 2016, 569-570, 619-626.	8.0	104
13	Optimizing a Parameterized Plug-and-Play ADMM for Iterative Low-Dose CT Reconstruction. IEEE Transactions on Medical Imaging, 2019, 38, 371-382.	8.9	101
14	Learning Discriminative Part Detectors for Image Classification and Cosegmentation. , 2013, , .		92
15	Unpaired Brain MR-to-CT Synthesis Using a Structure-Constrained CycleGAN. Lecture Notes in Computer Science, 2018, , 174-182.	1.3	86
16	Model-driven deep-learning. National Science Review, 2018, 5, 22-24.	9.5	84
17	Unsupervised MR-to-CT Synthesis Using Structure-Constrained CycleGAN. IEEE Transactions on Medical Imaging, 2020, 39, 4249-4261.	8.9	79
18	Investigation of Primary and Secondary Particulate Brown Carbon in Two Chinese Cities of Xi'an and Hong Kong in Wintertime. Environmental Science & Technology, 2020, 54, 3803-3813.	10.0	63

#	Article	IF	CITATIONS
19	Sustainable ex-situ remediation of contaminated sediment: A review. Environmental Pollution, 2021, 287, 117333.	7.5	58
20	Optical source profiles of brown carbon in size-resolved particulate matter from typical domestic biofuel burning over Guanzhong Plain, China. Science of the Total Environment, 2018, 622-623, 244-251.	8.0	56
21	Parent, alkylated, oxygenated and nitrated polycyclic aromatic hydrocarbons in PM2.5 emitted from residential biomass burning and coal combustion: A novel database of 14 heating scenarios. Environmental Pollution, 2021, 268, 115881.	7.5	52
22	Emission factors, characteristics, and gas-particle partitioning of polycyclic aromatic hydrocarbons in PM2.5 emitted for the typical solid fuel combustions in rural Guanzhong Plain, China. Environmental Pollution, 2021, 286, 117573.	7.5	48
23	Flash Cut: Foreground Extraction with Flash and No-flash Image Pairs. , 2007, , .		47
24	Volatile organic compounds emissions from traditional and clean domestic heating appliances in Guanzhong Plain, China: Emission factors, source profiles, and effects on regional air quality. Environment International, 2019, 133, 105252.	10.0	41
25	Source, health risk and composition impact of outdoor very fine particles (VFPs) to school indoor environment in Xi'an, Northwestern China. Science of the Total Environment, 2018, 612, 238-246.	8.0	36
26	Parent, alkylated, oxygenated and nitro polycyclic aromatic hydrocarbons from raw coal chunks and clean coal combustion: Emission factors, source profiles, and health risks. Science of the Total Environment, 2020, 721, 137696.	8.0	35
27	Training Networks in Null Space of Feature Covariance for Continual Learning. , 2021, , .		34
28	Particle size distribution and air pollution patterns in three urban environments in Xi'an, China. Environmental Geochemistry and Health, 2015, 37, 801-812.	3.4	31
29	Personal exposure to PM2.5-bound organic species from domestic solid fuel combustion in rural Guanzhong Basin, China: Characteristics and health implication. Chemosphere, 2019, 227, 53-62.	8.2	31
30	The oxidative capacity of indoor source combustion derived particulate matter and resulting respiratory toxicity. Science of the Total Environment, 2021, 767, 144391.	8.0	31
31	Cytotoxicity of stabilized/solidified municipal solid waste incineration fly ash. Journal of Hazardous Materials, 2022, 424, 127369.	12.4	29
32	Light absorption properties and molecular profiles of HULIS in PM2.5 emitted from biomass burning in traditional "Heated Kang―in Northwest China. Science of the Total Environment, 2021, 776, 146014.	8.0	27
33	Indoor secondary organic aerosols formation from ozonolysis of monoterpene: An example of d-limonene with ammonia and potential impacts on pulmonary inflammations. Science of the Total Environment, 2017, 579, 212-220.	8.0	26
34	Effects of domestic solid fuel combustion emissions on the biomarkers of homemakers in rural areas of the Fenwei Plain, China. Ecotoxicology and Environmental Safety, 2021, 214, 112104.	6.0	26
35	Neural multi-atlas label fusion: Application to cardiac MR images. Medical Image Analysis, 2018, 49, 60-75.	11.6	25
36	Characterization of polycyclic aromatic hydrocarbon (PAHs) source profiles in urban PM2.5 fugitive dust: A large-scale study for 20 Chinese cites. Science of the Total Environment, 2019, 687, 188-197.	8.0	25

#	Article	IF	CITATIONS
37	Characteristics and source apportionment of winter black carbon aerosols in two Chinese megacities of Xi'an and Hong Kong. Environmental Science and Pollution Research, 2018, 25, 33783-33793.	5.3	24
38	Environmental and health risks of VOCs in the longest inner–city tunnel in Xi'an, Northwest China: Implication of impact from new energy vehicles. Environmental Pollution, 2021, 282, 117057.	7.5	23
39	Learning Dictionary of Discriminative Part Detectors for Image Categorization and Cosegmentation. International Journal of Computer Vision, 2016, 120, 111-133.	15.6	21
40	Unsupervised Domain Adaptation with Regularized Optimal Transport for Multimodal 2D+3D Facial Expression Recognition. , 2018, , .		20
41	Explorations of tire and road wear microplastics in road dust PM2.5 at eight megacities in China. Science of the Total Environment, 2022, 823, 153717.	8.0	20
42	Cytotoxicity and Potential Pathway to Vascular Smooth Muscle Cells Induced by PM _{2.5} Emitted from Raw Coal Chunks and Clean Coal Combustion. Environmental Science & Technology, 2020, 54, 14482-14493.	10.0	19
43	Oxidative stress–inducing effects of various urban PM2.5 road dust on human lung epithelial cells among 10 Chinese megacities. Ecotoxicology and Environmental Safety, 2021, 224, 112680.	6.0	16
44	Joint Depth and Defocus Estimation From a Single Image Using Physical Consistency. IEEE Transactions on Image Processing, 2021, 30, 3419-3433.	9.8	15
45	Characterization of organic aerosols in PM1 and their cytotoxicity in an urban roadside area in Hong Kong. Chemosphere, 2021, 263, 128239.	8.2	13
46	Variations of Personal Exposure to Particulate Nitrated Phenols from Heating Energy Renovation in China: The First Assessment on Associated Toxicological Impacts with Particle Size Distributions. Environmental Science & Technology, 2022, 56, 3974-3983.	10.0	12
47	Scale selection for anisotropic diffusion filter by Markov random field model. Pattern Recognition, 2010, 43, 2630-2645.	8.1	11
48	Size distribution, community composition, and influencing factors of bioaerosols on haze and non-haze days in a megacity in Northwest China. Science of the Total Environment, 2022, 838, 155969.	8.0	11
49	A Model-Driven Deep Dehazing Approach by Learning Deep Priors. IEEE Access, 2021, 9, 108542-108556.	4.2	10
50	Aerosols chemical composition, light extinction, and source apportionment near a desert margin city, Yulin, China. PeerJ, 2020, 8, e8447.	2.0	9
51	Source profiles of molecular structure and light absorption of PM2.5 brown carbon from residential coal combustion emission in Northwestern China. Environmental Pollution, 2022, 299, 118866.	7.5	9
52	Saccharides Emissions from Biomass and Coal Burning in Northwest China and Their Application in Source Contribution Estimation. Atmosphere, 2021, 12, 821.	2.3	8
53	Profiles and Source Apportionment of Nonmethane Volatile Organic Compounds in Winter and Summer in Xi'an, China, based on the Hybrid Environmental Receptor Model. Advances in Atmospheric Sciences, 2021, 38, 116-131.	4.3	8
54	Evaluation on exposures to particulate matter at a junior secondary school: a comprehensive study on health risks and effective inflammatory responses in Northwestern China. Environmental Geochemistry and Health, 2018, 40, 849-863.	3.4	7

#	Article	IF	CITATIONS
55	Loss of E-cadherin due to road dust PM2.5 activates the EGFR in human pharyngeal epithelial cells. Environmental Science and Pollution Research, 2021, 28, 53872-53887.	5.3	7
56	Xâ€ray pulsar navigation using multiple detectors based on a new observation strategy. IET Radar, Sonar and Navigation, 2018, 12, 442-448.	1.8	6
57	Second-Order Spectral Transform Block for 3D Shape Classification and Retrieval. IEEE Transactions on Image Processing, 2020, 29, 4530-4543.	9.8	6
58	An Improved 3D Shape Recognition Method Based on Panoramic View. Mathematical Problems in Engineering, 2018, 2018, 1-11.	1.1	5
59	Pulsar/Star Tracker/INS Integrated Navigation Method Based on Asynchronous Observation Model. Journal of Aerospace Engineering, 2019, 32, 04019075.	1.4	5
60	Spatial Distribution, Source Apportionment, Ozone Formation Potential, and Health Risks of Volatile Organic Compounds over a Typical Central Plain City in China. Atmosphere, 2020, 11, 1365.	2.3	5
61	Learning Distribution Independent Latent Representation for 3D Face Disentanglement. , 2020, , .		3
62	Real-time chemical composition of ambient fine aerosols and related cytotoxic effects in human lung epithelial cells in an urban area. Environmental Research, 2022, 209, 112792.	7.5	3
63	Data Acquisition Method of Sensor News Based on Collaborative Filtering Algorithm. Wireless Communications and Mobile Computing, 2022, 2022, 1-9.	1.2	2
64	Variational HyperAdam: A Meta-learning Approach to Network Training. IEEE Transactions on Pattern Analysis and Machine Intelligence, 2021, PP, 1-1.	13.9	1
65	PM2.5 causes vascular hyperreactivity through the upregulation of the thromboxane A2 receptor and activation of MAPK pathways. Environmental Science and Pollution Research, 2022, , 1.	5.3	1
66	Learning Polynomial-Based Separable Convolution for 3D Point Cloud Analysis. Sensors, 2021, 21, 4211.	3.8	0
67	An Interpretable Early Dynamic Sequential Predictor for Sepsis-Induced Coagulopathy Progression in the Real-World Using Machine Learning. Frontiers in Medicine, 2021, 8, 775047.	2.6	0